Printed ISSN 1330–0016
Online ISSN 1333–9133
CD ISSN 1333–8390
CODEN FIZBE7

SPIN OBSERVABLES IN PION PHOTOPRODUCTION FROM A UNITARY AND CAUSAL EFFECTIVE FIELD THEORY

A. M. GASPARYAN[a,b] and M. F. M. LUTZ[a]

[a]*GSI Helmholtzzentrum für Schwerionenforschung GmbH, Planckstrasse 1, 64291 Darmstadt, Germany*

[b]*SSC RF ITEP, Bolshaya Cheremushkinskaya 25, 117218 Moscow, Russia*

Received 29 December 2010; Revised manuscript received 24 November 2011
Accepted 17 December 2011 Online 4 January 2012

Pion photoproduction is analyzed with the chiral Lagrangian. Partial-wave amplitudes are obtained by an analytic extrapolation of sub-threshold reaction amplitudes computed in chiral perturbation theory, where the constraints set by electromagnetic-gauge invariance, causality and unitarity are used to stabilize the extrapolation. The experimental data set is reproduced up to energies $\sqrt{s} \simeq 1300$ MeV in terms of the parameters relevant at order Q^3. We present and discuss predictions for various spin observables.

PACS numbers: 13.60.Le, 11.30.Rd UDC 539.126, 539.122

Keywords: pion photoproduction, chiral perturbation theory, stabilization of extrapolation, spin observables

1. Introduction

Chiral perturbation theory is a systematic tool for studying low-energy hadron dynamics. Particularly pion-nucleon scattering and pion photoproduction were considered in Refs. [1 − 5]. The application of χPT is however limited to the near threshold region. A method to extrapolate χPT results beyond the threshold region using analyticity and unitarity constraints was proposed recently in Ref. [6]. We focus on results obtained for pion photoproduction. The predictions for spin observables as currently measured at MAMI are confronted with previous theoretical predictions.

2. Chiral symmetry, causality and unitarity

Our approach is based on the chiral Lagrangian involving pion, nucleon and photon fields [5, 3]. The terms relevant at the order Q^3 for pion elastic scattering and pion photoproduction are listed below[1]

$$
\begin{aligned}
\mathcal{L}_{int} \;=\; & -\frac{1}{4\,f^2}\,\bar{N}\,\gamma^\mu\,\big(\boldsymbol{\tau}\cdot\big(\boldsymbol{\pi}\times(\partial_\mu\boldsymbol{\pi})\big)\big)\,N+\frac{g_A}{2\,f}\,\bar{N}\,\gamma_5\,\gamma^\mu\,\big(\boldsymbol{\tau}\cdot(\partial_\mu\boldsymbol{\pi})\big)\,N \\
- \;& e\Big\{\big(\boldsymbol{\pi}\times(\partial_\mu\boldsymbol{\pi})\big)_3+\bar{N}\,\gamma_\mu\,\frac{1+\tau_3}{2}\,N-\frac{g_A}{2\,f}\,\bar{N}\,\gamma_5\,\gamma_\mu\,\big(\boldsymbol{\tau}\times\boldsymbol{\pi}\big)_3\,N\Big\}\,A^\mu \\
- \;& \frac{e}{4\,m_N}\,\bar{N}\,\sigma_{\mu\nu}\,\frac{\kappa_s+\kappa_v\,\tau_3}{2}\,N\,F^{\mu\nu}+\frac{e^2}{32\pi^2 f}\,\epsilon^{\mu\nu\alpha\beta}\,\pi_3\,F_{\mu\nu}\,F_{\alpha\beta} \\
- \;& \frac{2\,c_1}{f^2}\,m_\pi^2\,\bar{N}\,(\boldsymbol{\pi}\cdot\boldsymbol{\pi})\,N-\frac{c_2}{2\,f^2\,m_N^2}\,\Big\{\bar{N}\,(\partial_\mu\,\boldsymbol{\pi})\cdot(\partial_\nu\boldsymbol{\pi})\,(\partial^\mu\partial^\nu N)+\text{h.c.}\Big\} \\
+ \;& \frac{c_3}{f^2}\,\bar{N}\,(\partial_\mu\,\boldsymbol{\pi})\cdot(\partial^\mu\boldsymbol{\pi})\,N-\frac{c_4}{2\,f^2}\,\bar{N}\,\sigma^{\mu\nu}\,\big(\boldsymbol{\tau}\cdot\big((\partial_\mu\boldsymbol{\pi})\times(\partial_\nu\boldsymbol{\pi})\big)\big)\,N \\
- \;& \mathrm{i}\,\frac{d_1+d_2}{f^2\,m_N}\,\bar{N}\,\big(\boldsymbol{\tau}\cdot\big((\partial_\mu\boldsymbol{\pi})\times(\partial_\nu\partial_\mu\boldsymbol{\pi})\big)\big)\,(\partial^\nu N)+\text{h.c.} \\
+ \;& \frac{\mathrm{i}\,d_3}{f^2\,m_N^3}\,\bar{N}\,\big(\boldsymbol{\tau}\cdot\big((\partial_\mu\boldsymbol{\pi})\times(\partial_\nu\partial_\lambda\boldsymbol{\pi})\big)\big)\,(\partial^\nu\partial^\mu\partial^\lambda N)+\text{h.c.} \\
- \;& 2\,\mathrm{i}\,\frac{m_\pi^2\,d_5}{f^2\,m_N}\,\bar{N}\,\big(\boldsymbol{\tau}\cdot\big(\boldsymbol{\pi}\times(\partial_\mu\boldsymbol{\pi})\big)\big)\,(\partial^\mu N)+\text{h.c.} \\
- \;& \frac{\mathrm{i}\,e}{f\,m_N}\,\epsilon^{\mu\nu\alpha\beta}\,\bar{N}\,\big(d_8\,(\partial_\alpha\,\pi_3)+d_9\,\big(\boldsymbol{\tau}\cdot(\partial_\alpha\boldsymbol{\pi})\big)\big)\,(\partial_\beta\,N)\,F_{\mu\nu}+\text{h.c.} \\
+ \;& \mathrm{i}\,\frac{d_{14}-d_{15}}{2\,f^2\,m_N}\,\bar{N}\,\sigma^{\mu\nu}\,\big((\partial_\nu\boldsymbol{\pi})\cdot(\partial_\mu\partial_\lambda\boldsymbol{\pi})\big)\,(\partial^\lambda N)+\text{h.c.} \\
- \;& \frac{m_\pi^2\,d_{18}}{f}\,\bar{N}\,\gamma_5\,\gamma^\mu\,\big(\boldsymbol{\tau}\cdot(\partial_\mu\boldsymbol{\pi})\big)\,N-\frac{e\,m_\pi^2\,d_{18}}{f}\,\bar{N}\,\gamma_5\,\gamma^\mu\,\big(\boldsymbol{\tau}\times\boldsymbol{\pi}\big)_3\,N\,A_\mu \\
+ \;& \frac{e\,(d_{22}-2\,d_{21})}{2\,f}\,\bar{N}\,\gamma_5\,\gamma^\mu\,\big(\boldsymbol{\tau}\times\partial^\nu\,\boldsymbol{\pi}\big)_3\,N\,F_{\mu\nu} \\
+ \;& \frac{e\,d_{20}}{2\,f\,m_N^2}\,\bar{N}\,\gamma_5\,\gamma^\mu\,\big(\boldsymbol{\tau}\times(\partial_\lambda\,\boldsymbol{\pi})\big)_3\,(\partial^\nu\partial^\lambda N)\,F_{\mu\nu}+\text{h.c.}\,.
\end{aligned}
\tag{1}
$$

A strict chiral expansion of the amplitude to the order Q^3 includes tree-level graphs, loop diagrams and counter terms. While the parameters $c_1 - c_4$ start to contribute at order Q^2, the terms with d's enter at the Q^3 order. The counter terms are adjusted to the empirical data on πN elastic scattering and pion photoproduction. The extrapolation of the amplitudes obtained within ChPT is performed utilizing constraints imposed by basic principles of analyticity and unitarity. For each partial wave, we solved the non-linear integral equation

[1] Note a typo in Eq. (1) of Ref. 6.

$$T_{ab}^{JP}(\sqrt{s}\,) = U_{ab}^{JP}(\sqrt{s}\,) + \sum_{c,d} \int_{\mu_{\rm thr}}^{\infty} \frac{{\rm d}w}{\pi} \frac{\sqrt{s}-\mu_M}{w-\mu_M} \frac{T_{ac}^{*,JP}(w)\,\rho_{cd}^{JP}(w)\,T_{db}^{JP}(w)}{w-\sqrt{s}-i\epsilon}\,, \tag{2}$$

where the generalized potential, $U_{ab}^{(JP)}(\sqrt{s}\,)$, is the part of the amplitude that contains left-hand cuts only. The phase-space matrix $\rho_{cd}^{JP}(w)$ reflects our particular convention for the partial-wave amplitudes, that are free of kinematical constraints. The subthreshold matching scale $\mu_M = m_N$ is required as to arrive at approximate crossing symmetric results. For more details we refer to Ref. [6].

3. Results

The low-energy constants relevant for the elastic pion-nucleon scattering were determined in Ref. [6]. The empirical s- and p-wave phase shifts are well reproduced up to the energy $\sqrt{s} \approx 1300$ MeV. Above this energy inelastic channels become important. The only exception is the P_{11} partial wave where the influence of inelastic channels is significantly larger, that results in a slightly worse description of the phase shift. A convincing convergence pattern was observed when going from Q^1 to Q^3 calculation. In addition to the low-energy constants of the Lagrangian (1) there are Castillejo-Dalitz-Dyson (CDD) pole parameters characterizing the Delta and Roper resonances [6].

The pion-photoproduction s- and p-wave multipoles are quite constrained. There are only four additional low-energy constants and four CDD-pole parameters for the twelve multipoles to be reproduced. Nevertheless, a good agreement to the existing partial wave analyzes was achieved. In order to avoid the ambiguities in the different partial-wave analyzes, we determined the parameters from the experimental data directly, where we excluded the near-threshold data in the fit. Our results for the differential cross sections, beam asymmetries and helicity asymmetry for the reaction channels $\gamma p \to \pi^0 p$, $\gamma p \to \pi^+ n$, $\gamma n \to \pi^- p$ are in agreement with experimental data from the threshold up to $\sqrt{s} = 1300$ MeV. Figure 1 confronts our prediction for the neutral pion-photo production with the near-threshold MAMI data [7, 8]. This data allows one to extract the electric s-wave multipole E_{0+}. Its energy dependence reveals a prominent cusp effect at the opening of the $\pi^+ n$ channel. As shown in Fig. 2, this structure is reproduced by our calculation, which discriminates the channels with neutral and charged pions.

Further information about the low-energy photoproduction dynamics is encoded in the p-wave threshold multipoles. In order to disentangle the three independent p-wave amplitudes, it is insufficient to measure the differential cross section only. The near-threshold beam asymmetry in $\gamma p \to \pi^0 p$ was measured by MAMI [8]. Our results are in striking disagreement with that measurement [6]. We predict the beam asymmetry to change sign close to threshold, in a similar manner as predicted before in the dynamical model of Kamalov et al. [9]. The results of Ref. [9] are also

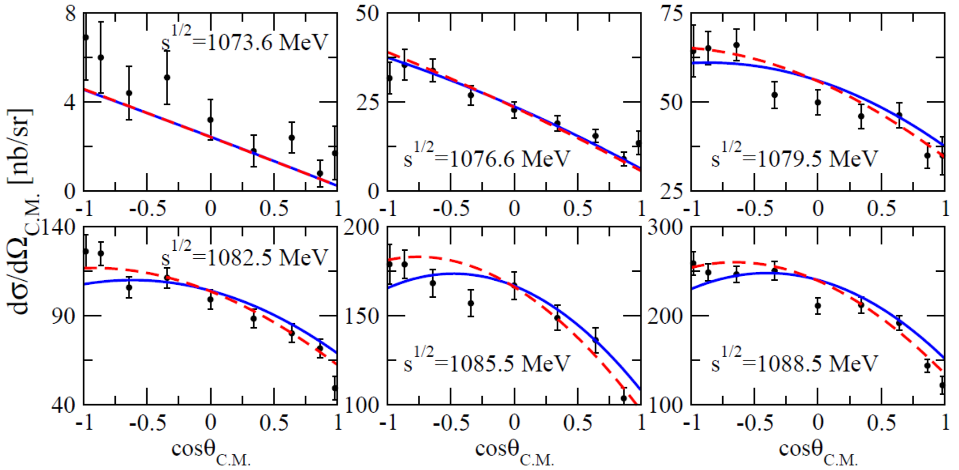

Fig. 1. Near-threshold differential cross sections for the reaction $\gamma p \to \pi^0 p$ with data taken from Refs. [7, 8]. Shown are results from our coupled-channel theory including isospin breaking effects as are implied by the use of empirical pion and nucleon masses. The solid lines correspond to our calculation with only s- and p-wave multipoles included. The effect of higher partial waves is shown by the dashed lines.

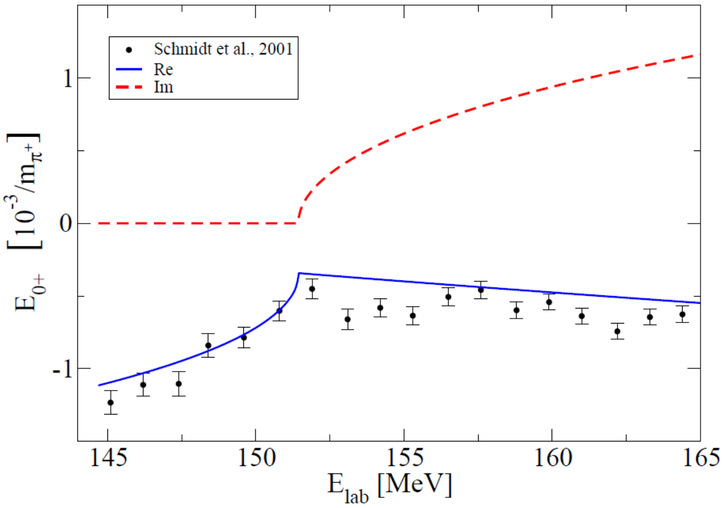

Fig. 2. Energy dependence of the E_{0+} multipole close to the pion production threshold. The data are from Ref. [8].

in conflict with the data obtained in Ref. [8]. In Fig. 3 we compare the two different results on the beam asymmetry. Though there is a qualitative agreement, important quantitative differences remain. It is interesting to observe that *d*-wave multipoles appear to play an important role in the near-threshold region. This was discussed

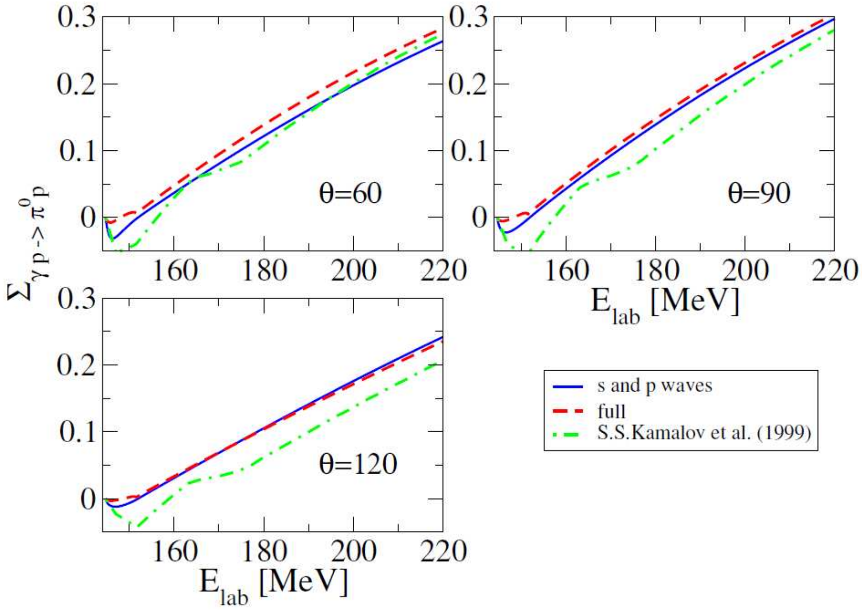

Fig. 3. Energy dependence of the beam asymmetry for three particular angles.

also in Ref. [10]. Thus the beam asymmetry may not be the optimal quantity to extract the p-wave threshold amplitudes. Currently a new data set on the beam asymmetry is being analyzed at MAMI.

We conclude that it is important to take further data on spin observables other than the beam asymmetry. Two cases are currently been studied at MAMI close to the threshold: the target asymmetry T and the double polarization observable F. Since there are different phase conventions used in the literature, the reader may appreciate that we detail the relevant expression in the convention used in Ref. [6], It holds

$$
\begin{aligned}
\frac{d\sigma}{d\Omega} &= \frac{\bar{p}_{\rm cm}}{2\,p_{\rm cm}} \left(|H_N|^2 + |H_{SA}|^2 + |H_{SP}|^2 + |H_D|^2\right) , \\
\Sigma\,\frac{d\sigma}{d\Omega} &= \frac{\bar{p}_{\rm cm}}{p_{\rm cm}}\, \Re\left(H_{SP}H_{SA}^* - H_N H_D^*\right) , \\
T\,\frac{d\sigma}{d\Omega} &= \frac{\bar{p}_{\rm cm}}{p_{\rm cm}}\, \Im\left(H_{SP}H_N^* + H_D H_{SA}^*\right) , \\
F\,\frac{d\sigma}{d\Omega} &= \frac{\bar{p}_{\rm cm}}{p_{\rm cm}}\, \Re\left(H_{SP}H_N^* + H_D H_{SA}^*\right) , \qquad (3)
\end{aligned}
$$

with $x = \cos\theta$ and

$$
H_N = \frac{m_N}{4\pi\sqrt{s}} \cos\frac{\theta}{2} \sum_J \left(t^J_{+,1} - t^J_{-,1}\right) \left(P'_{J+\frac{1}{2}}(x) - P'_{J-\frac{1}{2}}(x)\right) ,
$$

$$H_{SA} = -\frac{m_N}{4\pi\sqrt{s}} \sin\frac{\theta}{2} \sum_J \left(t^J_{+,1} + t^J_{-,1}\right) \left(P'_{J+\frac{1}{2}}(x) + P'_{J-\frac{1}{2}}(x)\right) ,$$

$$H_{SP} = \frac{m_N}{4\pi\sqrt{s}} \frac{-\sin\theta\cos\frac{\theta}{2}}{\sqrt{(J-\frac{1}{2})(J+\frac{3}{2})}} \sum_J \left(t^J_{+,2} - t^J_{-,2}\right) \left(P''_{J+\frac{1}{2}}(x) - P''_{J-\frac{1}{2}}(x)\right) ,$$

$$H_D = \frac{m_N}{4\pi\sqrt{s}} \frac{\sin\theta\sin\frac{\theta}{2}}{\sqrt{(J-\frac{1}{2})(J+\frac{3}{2})}} \sum_J \left(t^J_{+,2} + t^J_{-,2}\right) \left(P''_{J+\frac{1}{2}}(x) + P''_{J-\frac{1}{2}}(x)\right) .$$

In Fig. 4 and Fig. 5 we show our predictions at different angles for the energy dependence of the target asymmetry and the F observable in comparison with the predictions of the dynamical model of Ref. [9]. One can see that the target and beam asymmetry are most sensitive to the details of the dynamics, whereas the F observable is quite similar in both approaches.

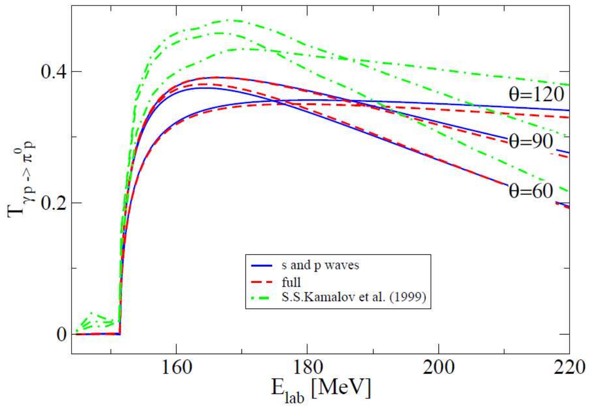

Fig. 4. Energy dependence of the target asymmetry for three particular angles.

In order to unravel the dynamics close to the threshold, we detail the contributions of s- and p-waves to the differential cross section and the Σ, T and F observables. They are

$$\begin{aligned}
\frac{d\sigma}{d\Omega} &= \frac{\bar{p}_{cm}}{p_{cm}} \Big[|E_{0+}|^2 + \frac{1}{2}|P_2|^2 + \frac{1}{2}|P_3|^2 + 2\,\Re(E_{0+}P_1^*)\cos\theta \\
&+ \Big(|P_1|^2 - \frac{1}{2}|P_2|^2 - \frac{1}{2}|P_3|^2\Big)\cos^2\theta\Big] , \\
\Sigma\frac{d\sigma}{d\Omega} &= \frac{\bar{p}_{cm}}{2\,p_{cm}} \big[\,|P_3|^2 - |P_2|^2\big]\sin^2\theta , \\
T\frac{d\sigma}{d\Omega} &= -\frac{\bar{p}_{cm}}{p_{cm}} \Im\big[(E_{0+} + P_1\cos\theta)(P_2 - P_3)^*\big]\sin\theta ,
\end{aligned}$$

$$F\,\frac{\mathrm{d}\sigma}{\mathrm{d}\Omega} \;=\; \frac{\bar{p}_{\rm cm}}{p_{\rm cm}}\,\Re\big[(E_{0+}+P_1\cos\theta)\,(P_2-P_3)^*\big]\,\sin\theta, \tag{4}$$

with the linear combinations of p-wave multipoles $P_1 = 3\,E_{1+} + M_{1+} - M_{1-}$, $P_2 = 3\,E_{1+} - M_{1+} + M_{1-}$, $P_3 = 2\,M_{1+} + M_{1-}$.

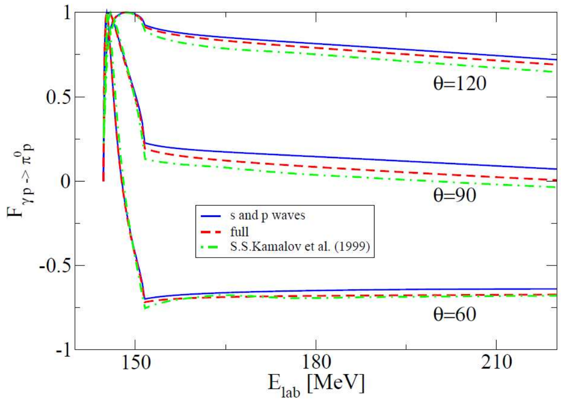

Fig. 5. Energy dependence of the double polarization observable F for three particular angles.

The expression for the target asymmetry T (Eq. (4)) depends on the imaginary parts of the multipoles. That is why close to the $\pi^0 p$ threshold, T is very small (see Fig. 4). Slightly above the $\pi^+ n$ threshold, it holds approximately

$$T\,\frac{\mathrm{d}\sigma}{\mathrm{d}\Omega}(\theta=90^\circ) \approx -\frac{\bar{p}_{\rm cm}}{p_{\rm cm}}\,\Im(E_{0+})\,(P_2-P_3)\,, \tag{5}$$

since the imaginary parts of p-wave multipoles are small. The imaginary part of E_{0+} is in turn dominated by the intermediate $\pi^+ n$ state. This allows one to access the difference $P_2 - P_3$ in the vicinity of the $\pi^+ n$ threshold.

In the beam asymmetry Σ, the p-waves multipoles enter only quadratically, and therefore the terms containing an interference of the E_{0+} and d-wave amplitudes are not suppressed by powers of the πN momentum. Moreover, the magnitudes of $|P_2|$ and $|P_3|$ are similar [8] which further diminishes the relative importance of the p-wave contribution to Σ. In contrast, the quantity $F(\theta = 90^\circ)$ contains the term $\Re(E_{0+}\,(P_2 - P_3)^*)$ but no other competing contribution. For a discussion of the importance of higher partial waves for different observables see also Ref. [10]. We conclude that a direct measurement of F provides a reliable determination of $P_2 - P_3$. Note that this difference is not small because P_2 and P_3 have opposite signs [8].

4. Summary

We studied pion photoproduction from threshold up to $\sqrt{s} = 1300$ MeV with a novel approach developed in Ref. [6], based on an analytic extrapolation of subthreshold amplitudes calculated in ChPT. The free parameters were adjusted to the pion-nucleon and photoproduction empirical data excluding the threshold region. Nevertheless, the near-threshold MAMI data on the differential cross section for the reaction $\gamma p \to \pi^0 p$ are described well. The energy dependence of the s-wave electric E_{0+} multipole close to the threshold, including its prominent cusp structure, is also well reproduced. We present predictions for the spin observables that are planned to be measured or being analyzed at MAMI. Our predictions are compared with results of the dynamical model of Kamalov et al. [9]. The importance of d-waves for the beam asymmetry close to the πN threshold is emphasized. This effect indicates that the beam asymmetry may be not best suited to disentangle the various p-wave threshold multipoles as has been anticipated before. We argue that the measurement of the double-polarization observable F suits this purpose much better.

Acknowledgements

We thank M. Ostrick and L. Tiator for stimulating discussions.

References

[1] V. Bernard, N. Kaiser and U.-G. Meissner, Int. J. Mod. Phys. E **4** (1995) 193.

[2] V. Bernard, N. Kaiser and U.-G. Meissner, Eur. Phys. J. A **11** (2001) 209.

[3] V. Bernard, Prog. Part. Nucl. Phys. **60** (2008) 82.

[4] V. Bernard, N. Kaiser and U.-G. Meissner, Nucl. Phys. A **615** (1997) 483.

[5] N. Fettes, U.-G. Meissner and S. Steininger, Nucl. Phys. A **640** (1998) 199.

[6] A. Gasparyan and M. Lutz, Nucl. Phys. A **848** (2010) 126.

[7] A. Schmidt, PhD thesis, Mainz (2001), http://wwwa2.kph.unimaiz.de/A2/.

[8] A. Schmidt et al., Phys. Rev. Lett. **87** (2001) 232501.

[9] S. S. Kamalov, G.-Y. Chen, S.-N. Yang, D. Drechsel and L. Tiator, Phys. Lett. B **522** (2001) 27.

[10] C. Fernandez-Ramirez, A. M. Bernstein and T. W. Donnelly, Phys. Rev. C **80** (2009) 065201.

SPINSKE MJERNE VELIČINE U FOTOTVORBI PIONA NA OSNOVI UNITARNE I KAUZALNE EFEKTIVNE TEORIJE POLJA

Kiralnim langranžijanom analiziramo pionsku fototvorbu. Amplitude parcijalnih valova smo dobili analitičkom ekstrapolacijom amplituda ispod praga reakcija, izračunatih u kiralnoj teoriji smetnje, a za stabilizaciju ekstrapolacije smo primijenili ograničenja postavljena elektromagnetskom baždarnom invarijancijom, kauzalnošću i unitarnošću. Postižemo sklad s mjernim podacima do energija $\sqrt{s} \simeq 1300$ MeV s članovima u parametrima važnim do reda Q^3. Predstavljamo i raspravljamo predviđanja za razne spinske opservable.